Journal of Mines, Metals and Fuels, *70(7) : 380-394; 2022. DOI: 10.18311/jmmf/2022/31962*

Print ISSN : 0022-2755

Journal of Mines, Metals and Fuels

Contents available at: www.informaticsjournals.com/index.php/jmmf

Influence of Alloying Element and Ageing on Microstructure and Dry Sliding Wear Behaviour of Cu-Zn-xNi Alloy

A. N. Santhosh[1*], S. Aprameyan[1], Suresh Erannagari[2] and Vasantha Kumar[3]

[1]Department of Mechanical Engineering, C Byregowda Institute of Technology, Kolar – 563101, Karnataka, India; ansanthoshan@gmail.com
[2]Department of Mechanical Engineering, BMSCE, Bengaluru – 560019, Karnataka, India
[3]Department of Mechanical Engineering, Bearys Institute of Technology, Mangalore – 574153, Karnataka, India

Abstract

In this paper, we look at how different nickel concentrations (4, 8, and 12 percent) affect the microstructure, microhardness, and dry sliding wear behaviour of a Cu-Zn-xNi alloy. The alloy was created using a casting technique at 1100°C and a heat treatment method that included solution treatment at 600°C and ageing at 450°C for four hours each. Microstructure studies were performed on the developed alloys using a scanning electron microscope (SEM). To investigate alloy indentation resistance, an ASTM E384 microhardness test was performed. Tribological properties such as friction and wear were investigated using a pin on disc tribometer and a dry sliding wear test according to the ASTM G99 standard. SEM studies revealed α-phase (copper) and solid solution of zinc in cast alloys, while aged alloys revealed a similar structure but with the addition of Cu2NiZn precipitates. The microhardness values improved as the Ni content and ageing increased. The decrease in secondary dendrite arm spacing with increasing Ni content and ageing was attributed to the improvement. The coefficient of friction decreased as the load increased, but increased as the sliding velocity increased. However, as loads and sliding velocities increased, so did the wear rate. For the majority of loads and sliding velocities, the worn surface demonstrated abrasion as the dominant wear mechanism.

Keywords: *Brass, Casting, Friction, Microstructure, Microhardness, Wear*

1. Introduction

Copper and it alloys are well known for their high thermal and electrical conductivity and in addition they possess good corrosion resistance and mechanical properties. As a result of the formation of intermetallic compounds when copper is alloyed with the elements IIB – IVB group, its properties change significantly. Because of their excellent corrosion resistance, machinability, and formability, solid-solution alloys such as copper-zinc (Cu-Zn) alloys are the most commonly used copper alloys. The phases of technical interest are α-phase (FCC) and α-phase (BCC), but intermetallic content with high Zn content is irrelevant (Freudenberger *et al.*, 2018). Intricate shapes can be fabricated using deep drawing and a Cu-Zn alloy with greater strength than pure copper. However,

**Author for correspondence*

malleability is highly dependent on zinc content, and if it is greater than 45 percent, it cannot be worked in either hot or cold conditions. The most important aspect is that, in comparison to pure copper, Cu-Zn alloys have greater elongation and strength. Hardness and strength can be increased further by ageing the alloys, which results in the formation of several intermetallic compounds such as and'. Brass has a melting point of 900°C to 940°C and is classified as alpha brass, beta brass, or duplex brass based on its zinc content. Engineering pumps, tanks, screws, terminal blocks, panel board switches, sprinkler heads, window fittings, door fittings, base plates, and gear metres are all made from brass. Furthermore, the low friction properties and durability of this alloy make it an ideal candidate for mechanical components such as valves, bearings, ammunition cartridge cases, and gears (Davis *et al.*, 2001; Stewart, 2021).

We have seen that copper and its alloys are quite unique in terms of electrical and thermal properties, but they also have certain other unique characteristics such as wear resistance and a self-lubrication mechanism (Prasad, 1997; Davim, 2000). Sadykov *et al.* (1999) investigated the effect of various factors on the wear properties of copper and its alloys. Commercial purity copper alloys, Cu-Al-Fe alloys, and Cu-Zn-Pb alloys were developed using cold working techniques. The wear test revealed that the Cu-Al-Fe alloy had a high wear intensity, whereas copper had a low wear intensity. The main focus of this work was the reduction in wear as the microstructure changed from dendrite to submicrocrystalline. Davim (2000) used a pin on disc test rig to investigate the tribological behaviour of brass against Ck45-DIN steel. The experiments were carried out using the Taguchi method, with three factors, each with three levels. The ANOVA analysis for coefficient of friction revealed that temperature was the most influential factor, while load was the least influential. Similarly, the load factor had the greatest influence on wear rate, while the velocity factor had the least. Unlu *et al.* (2009) used a radial wear setup to investigate the tribological properties of Cu-30Zn and Cu-10Sn alloys. Cu-30Zn and Cu-10Sn alloys had Brinell hardnesses of 120 and 100 HB, respectively. The bearing rate of both alloys was found to increase with time and to be higher for the Cu-30Zn alloy. The friction rate, on the other hand, was found to decrease with time and was highest for the Cu-10Sn alloy. Kucukomeroglu and Kara (2014) investigated the friction and wear properties of a Cu-39Zn-3Pb alloy under vacuum (510-3 mbar and 810-6 mbar) and atmospheric (1013 mbar) test conditions. The alloy had a low coefficient of friction at atmospheric pressure but a high coefficient of friction at 810-6 mbar pressure. The wear volume, however, was higher at atmospheric pressure and lower at 810-6 mbar pressure. The wear type determined by SEM analysis was abrasive in atmospheric conditions and adhesive in vacuum conditions. Moshkovich *et al.* (2014) published an interesting study on the friction and wear properties of copper and brass (/) in the presence of synthetic oil (PAO-4). The wear and coefficient of friction of brass were significantly higher than that of copper when tested against AISI 1040 steel. Surface studies revealed that copper friction in the boundary layer region resulted in the formation of nanocrystalline structures with grain sizes of about 100 nm. The formation of ultra-fine grain layers allowed copper to wear less and have a lower friction coefficient.

Other alloying elements, such as Ni, have significantly improved the mechanical properties of Cu-Zn alloy. Chen *et al.* (2017) investigated the impact of Ni and Si addition on the structure and mechanical behaviour of a Cu-Zn alloy. The 1.5 percent Ni added Cu-Zn was made using a casting technique, heat treatment at 900°C, rolling to reduce thickness by 80 percent, and finally ageing at 350°C. The addition of Ni and Si increased the hardness and tensile strength of the Cu-Zn alloy significantly, which was attributed to the formation of -Ni2Si precipitates. Wang *et al.* (2019) investigated the effect of cryogenic rolling on the structural and mechanical properties of a Cu-Zn alloy containing Ni and Si. The alloy, which contained 1.0 percent Ni and 0.2 percent Si, was created by rolling with a 90% reduction followed by annealing at 300°C. The tensile strength of Ni and Si added rolled alloy was 768.4 MPa, while the rolled alloy strength without alloying elements was 711.3 MPa. On a comparable scale, the Vickers hardness of Cu-Zn-Ni-Si was 253.7 HV, while Cu-Zn alloy was 234.5 HV. The formation of Ni_2Si precipitates played a significant role in improving tensile strength and ductility. In another study, Joszt *et al.* (1980) investigated the Ni-added Cu-Zn alloy when cold rolled and annealed at various temperatures. The rolling reduction with 90% reduction had the highest hardness, and the peak hardness was achieved at an annealing temperature of 573 K. Similarly, at 573 K and 90% reduction, the yield and ultimate tensile strength were found to be higher. The superlattice domain size of 4 nm indicates that there is significant resistance to dislocation

motion due to increased ordering, which resulted in higher yield strengths for 573 K annealing temperature and 90% rolling reduction. Apart from mechanical properties, Moussa *et al.* (2022) investigated the wear behaviour of a brass alloy containing 0.22 percent Ni, 0.43 percent Sn, 0.50 percent Al, and 1.61 percent Pb by weight. The wear test was carried out using an ASTM G99-05 pin on ring test rig, and the ring material was ball bearing steel with a hardness of 63 HRC. The weight loss increased from 0.04 g to 0.105 g as the load increased from 10 N to 50 N. The worn surface analysis revealed that lower loads experienced mild delamination wear, while higher loads experienced adhesive and delamination wear mechanisms. Other noticeable features of the worn surface included severe spalling, large plastic deformation, and cracks.

Following in the footsteps of previous published papers, this work focuses on the dry sliding wear behaviour of brass with varying nickel content. The effect of nickel on wear characteristics such as coefficient of friction and wear rate was investigated using an ASTM G 99 pin on disc test rig. Furthermore, the SEM was used to analyse the worn surface of cast and aged brass alloy samples, and the wear mechanism responsible for weight loss was proposed using micrographs.

2. Experimentation

In order to prepare the Cu-Zn-xNi alloy, the raw materials used were pure copper ingots (purity of 99.95%), Zn metal strips (purity of 99.5%) and Ni metal powder (purity of 99.5%). Here the weight percentage of Zn was fixed to 5% and Ni was varied from 4% to 12% in the step of 4%. A total mixture of 2000 g was made and based upon the percentage composition they were used for making alloy. The furnace charge calculated for each alloy is presented in the Table 1.

Based on the weight provided in the Table 1 the three different alloys with different content are produced via casting. Initially the copper ingots of were placed in the clay graphite crucible and the melting temperature was set to 1100°C. After complete melting the Ni was added to the melt and the temperature of the furnace was increased to 1500°C. At this stage to ensure uniform dispersion of Ni, the stirring of carried out with the mechanical stirrer. The hexachlorothane (C_2Cl_6) tablets were placed in the molten metal to remove entrapped gases. Further slag formed on the surface of melted was also removed to avoid pouring metal defects such as slag inclusion. In the final step the Zn was added to the molten metal followed by mixing with the help of mechanical stirrer. The molten metal was poured into the sand mould and allowed for solidification. Additional set of castings were made and subjected to solution treatment at temperature of 600°C for about 4 hours duration. This was followed by water quenching to room temperature and ageing at temperature of 450°C for about 4 hours duration.

Table 1. Furnace charge calculation for making Cu-Zn-xNi alloy

Composition	Copper, g	Zinc, g	Nickel, g
Cu - 5%Zn - 4%Ni alloy	1820	100	80
Cu - 5%Zn - 8%Ni alloy	1740	100	160
Cu - 5%Zn - 12%Ni alloy	1660	100	240

The cast and aged alloy samples were subjected polishing process for which SiC papers from 100 to 1500 grade were used. The final polishing process was conducted using diamond paste to obtain scratch free surface finish. The polished samples were scanning electron microscopy (Make: Tescan Vega3) for microstructure analysis. The microhardness test was carried out on each alloy as per ASTM E384 standard and load of 500 g was applied for a dwell time of 15 seconds. The average of nine indentations is reported as microhardness (HV) value of the alloy. The dry friction and wear test was carried out using pin on disc tribometer (Make: Ducom TR20-LE) as per ASTM G99 standard at ambient temperature. For this the alloys were machined to 6 mm diameter and 20 mm length with mating surface being polished to mirror finish having surface roughness value of 0.5 µm. The counterdisc selected for test was EN-31 steel which had hardness of HV 790 and surface roughness value of 0.9 µm. The load and sliding speed were applied in the range of 25 to 100 N and 0.314 to 1.256 m/s respectively. The worn surface of alloy samples were subjected to SEM (Make: Tescan Vega3) studies to study the worn mechanisms.

3. Results and Discussion

The effect of varying Ni content and ageing on microstructure, microhardness and tribological properties of Cu-Zn-xNi alloy is presented here.

3.1 Microstructure Studies

The SEM micrographs of Cu-Zn-xNi alloys in the cast and aged conditions are shown in the Figure 1 (a) – (f). The Cu-Zn-4Ni alloy, which contain lowest Ni content showed the dendrite structure for cast condition as observed in the Figure 1 (a). It is well known that pure copper is difficult to cast and in order to modify this behaviour it is alloyed with different metallic materials. The addition of alloying elements helps in enhancing the strength and elongation of pure copper. In this case with Zn was used as alloying element, the molten metal had got excellent fluidity and was poured above its freezing range without any complications. Since the alloy contains 5% zinc in copper, they are known as single phase alloys which mean the microstructure consist of α-phase (copper) and solid solution of zinc.

Because the α-phase (copper) crystal structure is face centred cubic, the solid solution has the same crystal structure. This SEM micrograph of a zinc α-phase and solid solution is consistent with the general observation described in previous publications (Davis *et al.*, 2001). However, the SEM micrograph of aged Cu-Zn-4Ni alloy shown in Figure 1 (b) revealed a very refined microstructure. The primary dendrite arm spacing in cast alloy is quite large, whereas in aged alloy the spacing is decreasing. The secondary dendrite arm spacing is a well-known solidified structure determinant. The distance between dendrite secondary arms in a solidified structure is referred to as secondary dendrite arm spacing. The distribution of impurities, intermediate phases, solutes, and eutectic phases is affected by dendrite size. It is simple to control the material's performance if one understands and controls the solidified structure via secondary dendrite arm spacing by studying its solidification conditions (Knych *et al.*, 2011; Yan *et al.*, 2013). As previously stated, the temperature gradient and solidification rate are the two factors that govern secondary dendrite arm spacing. The presence of Ni particles and the ageing process aided in the reduction of secondary dendrite arm spacing in aged Cu-Zn-4Ni alloy. This is the primary reason for aged alloy's refined microstructure when compared to cast alloy. Bagherian *et al.* (2016) investigated the microstructure of continuous cast Cu-Sn alloys with and without Zr as a grain refiner. The space between the secondary dendrite arms was found to be reduced by the addition of Zr, and precipitation resulted in significant refinement of dendrite grains. In a similar vein, Reis *et al.* (2013) investigated the effect of ageing time and dendritic arm spacing on the microhardness of an Al-Cu alloy. The dendritic arm spacing of the casting was measured in the longitudinal section of the Al-Cu casting from bottom to top. It was discovered that secondary dendrite arm spacing decreased after solution treatment and ageing. The hardness of the alloy increased as the average secondary dendrite arm spacing decreased. As a result, these findings support the claim that Ni addition and ageing can refine the microstructure of the Cu-Zn-4 Ni alloy, resulting in the formation of fine dendritic grains

When the Ni content was increased from 4% to 8%, the microstructure of the cast and aged alloys, as shown in Figure 1 (c) and (d), revealed the presence of α-phase (copper) and solid zinc solution, but dendrite refinement was still visible. The addition of more Ni has proven to be advantageous as the secondary dendrite arm spacing appears to be decreasing. The presence of more Ni allows for finer dendritic grains and a decrease in secondary dendrite arm spacing. This decrease in secondary dendrite arm spacing was also observed in (Bagherian *et al.*, 2016), where authors discovered that as Zr content increased from 2.6 to 6.8 percent, secondary dendrite arm spacing decreased from 4.65 to 1.54 m. As the Zr particle content increased, so did the number of nucleation sites for finer grains, resulting in a greater number of fine size dendritic grains. Furthermore, when compared to the cast alloy, the aged alloy had a slightly higher number of fine size dendritic grains, as shown in Figure 1 (d). Furthermore, certain dark coloured spots can be seen in the microstructure of aged Cu-Zn-8Ni alloy. The tiny spots are Cu2NiZn precipitates, according to the alloy's chemical composition. The number of Cu2NiZn precipitates in the aged Cu-Zn-4Ni alloy was significantly lower, as shown in Figure 1 (b), whereas higher Ni content resulted in a greater number of precipitates, which are visible in the microstructure as tiny dark spots. The steep thermal gradients favour thermodynamics of nucleation of fine dendrite grain formation as the alloy was subjected to solution treatment and ageing. Further ageing aided the diffusion kinetics, resulting in the formation of a clearly defined α-phase. The variation and distribution of phase were not significant, which could be beneficial in terms of microhardness. Furthermore, as the Ni content increased from 8% to 12%, the microstructure of the cast and aged alloys, as shown in Figure 1 (e) and (f), remained similar to that of previous alloys. The alloy contained α-phase (copper) and solid zinc solution, but dendrite refinement

was clearly visible. Ni content increase and ageing treatment resulted in microstructure refinement and the formation of fine dendrite grains. This observation is well supported by the work on heat treatment of lead-free

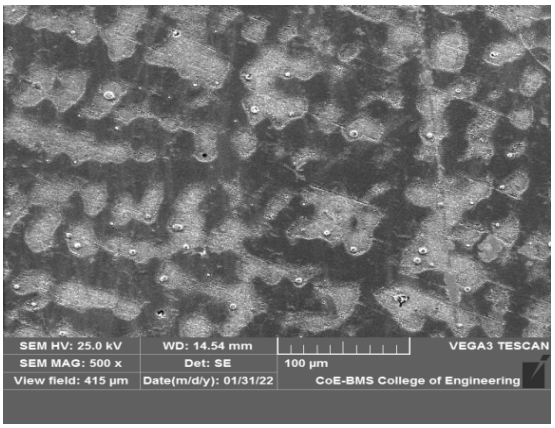

(a) Before Heat Treatment

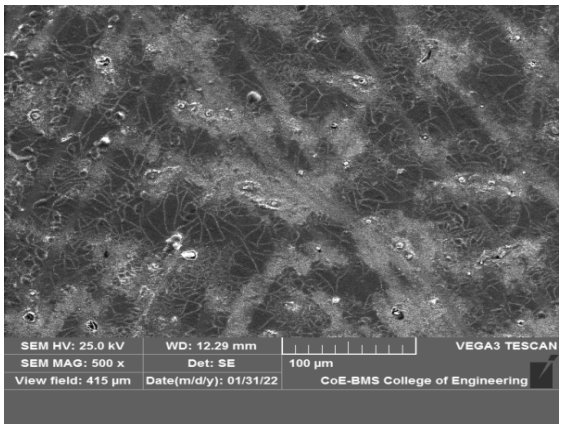

(b) After Heat Treatment

Copper+5%Zn+4%Ni

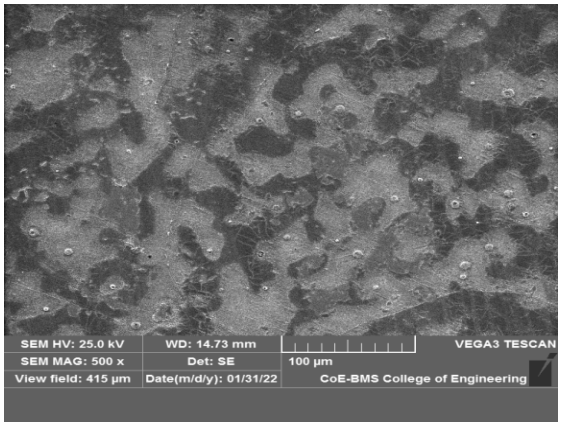

(c) Before Heat Treatment

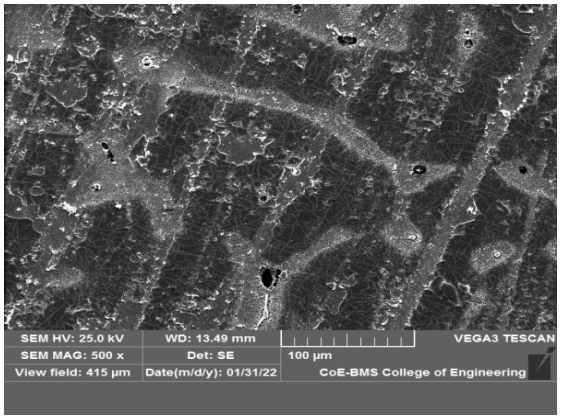

(d) After Heat Treatment

Copper+5%Zn+8%Ni

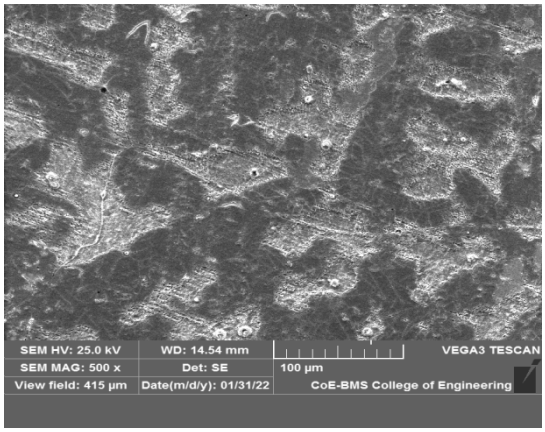

(e) Before Heat Treatment

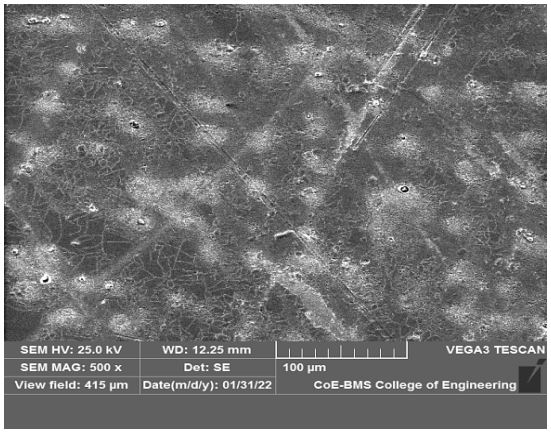

(f) After Heat Treatment

Copper+5%Zn+12%Ni

Figure 1. **(a-f).** SEM micrographs of Cu-Zn-xNi alloys.

brasses reported by Toulfatzis *et al.* (2020). Because steep thermal gradients favoured the nucleation process, higher soaking time and holding temperature were driving forces for precipitation. However, significant variation in the phase distribution was observed, affecting the mechanical properties. Overall, the microstructure analysis revealed that increasing the Ni content in cast and aged alloys aided in the formation of fine dendrite grains. When aged Cu-Zn-xNi alloys were compared to cast alloys, the effect of fine dendrite grain formation was more pronounced.

3.2 Microhardness Studies

Microhardness tests were performed on cast and aged Cu-Zn-xNi alloys, and the results were plotted as a function of Ni content, as shown in Figure 2. First, the microhardness value of the cast Cu-Zn-4Ni alloy was 76 VHN, and when the Ni content was increased to 8%, the microhardness value was 80 VHN. When the Ni content was increased from 4% to 8%, the percentage improvement in microhardness was approximately 5.2 percent. When we look at this value, it appears that the improvement was minor. Furthermore, increasing the Ni content from 8% to 12% resulted in a microhardness value of 85 VHN. When this value is compared to 4% and 8%, the percentage enhancement for Cu-Zn-12Ni alloy is approximately 11.8 percent and 6.2 percent. The alloy showed a significant increase in microhardness at 12% Ni content, which is attributed to microstructure refinement and the formation of fine dendrite grains. The microstructure of Cu-Zn-xNi alloys showed the presence of α-phase (copper) and solid solution of zinc, as shown in Figure 1 (a), (c), and (e), but most importantly, the structure was dendritic in nature. However, as the Ni content of the alloy increased from 4% to 8% and then to 12%, dendrite refinement occurred, as shown in Figure 1 (c) and (d) (e). To understand, we must first examine the basic microstructure of Cu-Zn alloys. Conventional casting produces α-phase and α-phase dendrites in Cu-Zn alloys with zinc contents greater than 25%. In such cases, the α-phase can be found in the interdendritic regions of the α-phase , or the α-phase can be said to separate the α-phase or dendrites. In such cases, the hardness and strength of the alloy increase as the Zn content increases. This is primarily due to the fact that α-phase is significantly harder and stronger than α-phase. However, in this case, the microstructure revealed a α-phase (copper) and a solid solution of zinc with no α-phase. This means that the hardness is solely determined by the Ni content, and that changes caused by Ni addition will affect the microhardness. From the standpoint of Ni content, it is quite clear that Ni addition resulted in microstructure refinement and the formation of fine dendrite grains. The presence of nickel, as well as an increase in its content, aided in the reduction of secondary dendrite arm spacing. The increase in Ni content from 4% to 12% resulted in a significant decrease in secondary dendrite arm spacing, as shown in Figure 1 (a), (c), and (e), allowing the alloys to achieve higher microhardness values.

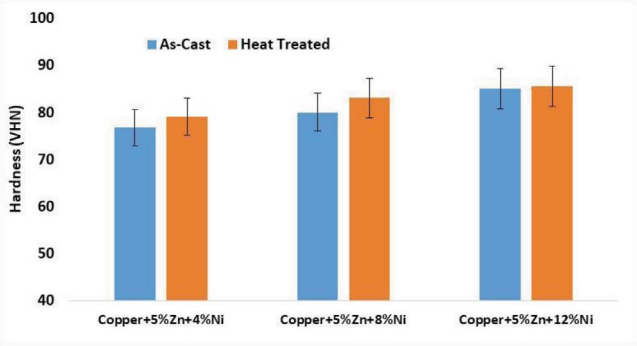

Figure 2. Variation of hardness in Cu-Zn-xNi alloys.

The microhardness value of aged Cu-Zn-4Ni alloy was determined to be 79 VHN, while increasing the Ni concentration to 8% enhanced the microhardness value to 83 VHN. As can be seen, increasing the Ni content increased the microhardness rating by around 5%. It appears that ageing process has resulted in marginal increase in the microhardness value. Further, increasing the Ni content from 8% to 12% resulted in value of 86 VHN. When this value is compared with those of Cu-Zn-4Ni alloy and Cu-Zn-8Ni alloy, the percentage enhancement is about 8.8% and 3.6% respectively. So with the increase in Ni content the aged samples showed considerable enhancement in the microhardness values. The reason for this behaviour is attributed to formation of Cu_2NiZn precipitates and fine dendrite grains. Both precipitates and fine grain boundaries enhance the microhardness by two factors restricting the grain boundary migration and inhibiting dislocation motion. Although one can observe that formation of Cu_2NiZn precipitates could have significantly contributed to the microhardness but here the observed improvement is marginal. Due to long ageing duration of 4 hours the precipitates grew to larger size such that there dislocation pinning ability is greatly minimized. In such scenario the dislocations

would experience much resistance from precipitates and move ahead after brief stop. The dislocations could either bypass or cut the precipitates which resulted in minor enhancement in the microhardness values of alloys. However, for Cu-Zn-12Ni alloy the presence of large number of Ni particles as nucleation sites the volume fraction of precipitates will be higher due to which it showed higher microhardness values compared to other two alloys. Similarly the addition of Ni particles led to significant refinement in dendritic structure as it was able to decrease the secondary dendrite arm spacing. As observed in the Figure 1 (b), (d) and (f), with the increase in Ni content from 4% to 12%, the secondary dendrite arm spacing is found to be decreasing. This helped in enhancing the microhardness of Cu-Zn-xNi alloys along with Cu_2NiZn precipitates. Correlating hardness with the secondary dendrite arm spacing, the Reis *et al.* (Reis *et al.*, 2013) reported a research work on Al-Cu alloys. The authors found that as the secondary dendrite arm spacing increased the hardness value was found to decreasing. This observation is well in line with the one made in this work however the trend is quite different as in present case the decrease in the secondary dendrite arm spacing led to enhancement in microhardness of Cu-Zn-xNi alloys. Now let's see the comparison between aged and cast alloys and how microhardness faired in these two conditions. The microhardness values of cast and aged Cu-Zn-4Ni alloy were 76 VHN and 79 VHN respectively. One can see that after ageing process the increase in the microhardness was about ~4%. Similarly the microhardness values of cast and aged Cu-Zn-8Ni alloy were 80 VHN and 83 VHN and the percentage increase in the microhardness was about ~3.8%. Finally, the microhardness values of cast and aged Cu-Zn-12Ni alloy were 85 VHN and 86 VHN and the percentage increase in the microhardness was about ~1.1%. Overall the compared to cast alloys, the aged alloys showed marginal increase in the microhardness and this was attributed to the formation of Cu_2NiZn precipitates (Jang and Hong, 2020; Igelegbai *et al.*, 2016; Toulfatzis *et al.*, 2016).

3.3 Coefficient of Friction

The coefficient of friction of cast Cu-Zn-xNi alloys was studied for varying load (25 N to 100 N) and sliding velocity (0.314 m/s to 1.256 m/s). Further the effect of heat treatment was also studied and compared with the values of cast alloys.

3.3.1 Effect of Load

The effect of Ni content on coefficient of friction of cast Cu-Zn-xNi alloys plotted as a function of varying load is presented in the Figure 3. First we will see the coefficient of friction values for Cu-Zn-4Ni alloy obtained at different loads from 25 N to 100 N. For Cu-Zn-4Ni alloy case the coefficient of friction was found to be decreasing with increasing load. In case of 25 N load, the coefficient of friction value was 0.56 and when the load was increased from 25 N to 50 N, the coefficient of friction value decreased to 0.515. The percentage decrement in the coefficient of friction when load was increased was about 8.03%. Similarly when the load was increased to 75 N and 100 N, the coefficient of friction values obtained were 0.49 and 0.35 respectively. Compared to 25 N, the decrement in the coefficient of friction was about 12.5% and 37.5% for 75 N and 100 N respectively. Overall low value of coefficient of friction was observed at higher load of 100 N and high value was obtained at lower load of 25 N. For Cu-Zn-8Ni alloy case the coefficient of friction was found to be decreasing with increasing load. At 25 N load, the coefficient of friction value was 0.435 and when the load was increased from 25 N to 50 N, the coefficient of friction value decreased to 0.40. The percentage decrement in the coefficient of friction when load was increased was about 8.04%. Similarly when the load was increased to 75 N and 100 N, the coefficient of friction values obtained were 0.36 and 0.30 respectively. Compared to 25 N, the decrement in the coefficient of friction was about 17.2% and 31% for 75 N and 100 N respectively. Overall low value of coefficient of friction was observed at higher load of 100 N and high value was obtained at lower load of 25 N. For Cu-Zn-12Ni alloy case the coefficient of friction was found to be decreasing with increasing load. At 25 N load, the coefficient of friction value was 0.415 and when the load was increased from 25 N to 50 N, the coefficient of friction value decreased to 0.355.

The percentage decrement in the coefficient of friction when load was increased was about 14.5%. Similarly, when the load was increased to 75 N and 100 N, the coefficient of friction values obtained were 0.32 and 0.28 respectively. Compared to 25 N, the decrement in the coefficient of friction was about 22.9% and 32.5% for 75 N and 100 N respectively. Overall low value of coefficient of friction was observed at higher load of 100 N and high value was obtained at lower load of 25 N. The presence of Zn in the alloy tends to decrease the coefficient of friction for all

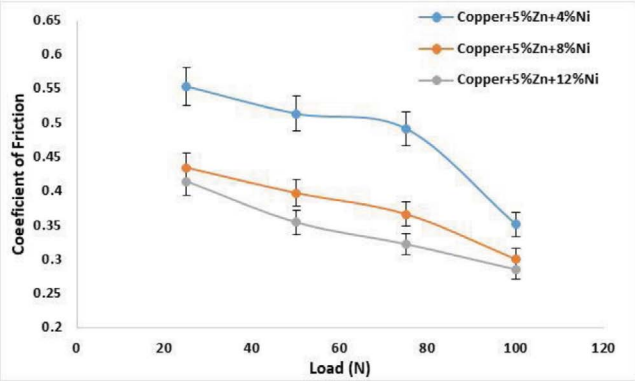

Figure 3. Effect of load on COF.

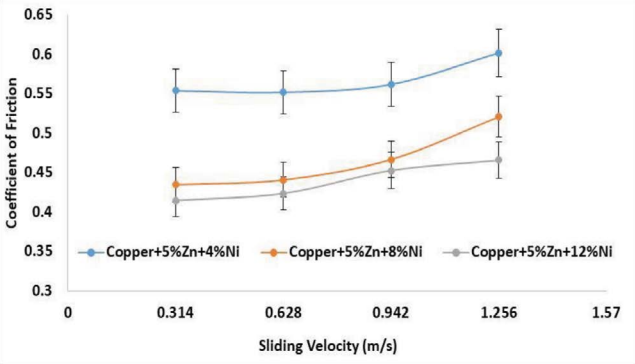

Figure 4. Effect of sliding velocity on COF.

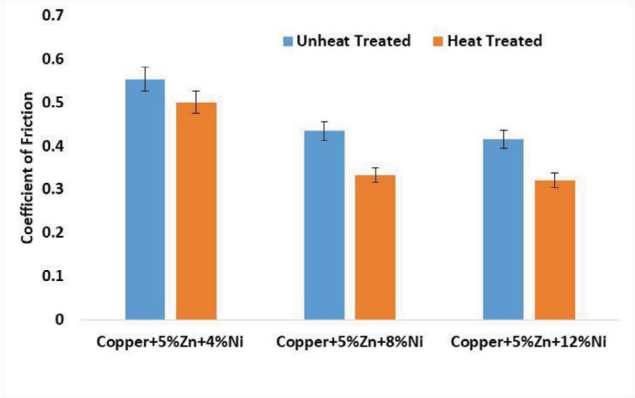

Figure 5. Effect of heat treatment on COF.

alloys. The crystal structure of α-phase is face centred cubic which implies that this phase possess high ductility while the Zn which as hexagonal close packed structure is known for its lubricating properties (Purcek *et al.*, 2002). Due to its crystal structure and ability to smear at high loads, the Zn helped the alloy to achieve lower coefficient of friction at higher loads.

3.3.2 Effect of Sliding Velocity

The effect of Ni content on coefficient of friction of cast Cu-Zn-xNi alloys plotted as a function of varying sliding velocity is presented in the Figure 4. First, we will see the coefficient of friction values for Cu-Zn-4Ni alloy obtained at different sliding velocity from 0.314 m/s to 1.256 m/s. For Cu-Zn-4Ni alloy case the coefficient of friction was found to be increasing with increasing sliding velocity. In case of 0.314 m/s sliding velocity, the coefficient of friction value was 0.55 and when the sliding velocity was increased from 0.314 m/s to 0.628 m/s, the coefficient of friction value was almost same without any noticeable changes. Similarly when the sliding velocity was increased to 0.942 m/s and 1.256 m/s, the coefficient of friction values obtained were 0.555 and 0.6 respectively. Compared to 0.314 m/s sliding velocity, the increment in the coefficient of friction was about ~1% and 9% for 0.942 m/s and 1.256 m/s respectively. Overall, the low value of coefficient of friction was observed at lower sliding velocity of 0.314 m/s and high value was obtained at higher sliding velocity of 1.256 m/s. For Cu-Zn-8Ni alloy case the coefficient of friction was found to be increasing with increasing sliding velocity. In case of 0.314 m/s sliding velocity, the coefficient of friction value was 0.44 and when the sliding velocity was increased from 0.314 m/s to 0.628 m/s, the coefficient of friction value was slightly increased to a value of 0.445. Similarly when the sliding velocity was increased to 0.942 m/s and 1.256 m/s, the coefficient of friction values obtained were 0.46 and 0.525 respectively. Compared to 0.314 m/s sliding velocity, the increment in the coefficient of friction was about ~4.5% and 19.3% for 0.942 m/s and 1.256 m/s respectively. Overall, the low value of coefficient of friction was observed at lower sliding velocity of 0.314 m/s and high value of coefficient of friction was obtained at higher sliding velocity of 1.256 m/s. Finally in case of Cu-Zn-12Ni alloy case the coefficient of friction was found to be increasing with increasing sliding velocity. In case of 0.314 m/s sliding velocity, the coefficient of friction value was 0.42 and when the sliding velocity was increased from 0.314 m/s to 0.628 m/s, the coefficient of friction value was slightly increased to a value of 0.43. Similarly when the sliding velocity was increased to 0.942 m/s and 1.256 m/s, the coefficient of friction values obtained were 0.45 and 0.46 respectively.

In comparison to 0.314 m/s sliding velocity, the coefficient of friction increased by approximately 7.1

percent and 9.5 percent at 0.942 m/s and 1.256 m/s, respectively. In general, a low coefficient of friction was observed at 0.314 m/s and a high coefficient of friction was reported at 1.256 m/s. Here it is seen that when the sliding velocity is increased the coefficient of friction of all alloys rise which can be attributed to rise in surface roughness of both the contact materials. At first, ploughing is modest due to the low sliding velocity, but as the sliding velocity increases, ploughing increases and so does the surface roughness. Both of these characteristics contribute to the increase in the coefficient of friction of all Cu-Zn-xNi alloys with increasing sliding velocity.

3.3.3 Effect of Heat Treatment

The effect of ageing on the coefficient of friction of cast Cu-Zn-xNi alloys was investigated, and the resulting value as a function of the Ni content is shown in Figure 5. The cast Cu-Zn-4Ni alloy had a coefficient of friction of 0.56, which reduced to 0.50 during ageing. When the aged alloy's coefficient of friction was compared to that of the cast alloy, a 10.7 percent decrease in value was observed. The coefficients of friction of cast and aged Cu-Zn-8Ni alloys, on the other hand, were found to be 0.43 and 0.33, respectively. Compared with cast alloy the percentage decrease in the coefficient of friction of aged Cu-Zn-8Ni alloy was about 23.2%. Finally in case of cast and aged Cu-Zn-12Ni alloy, the coefficient of friction values were 0.41 and 0.31 respectively. Compared with cast alloy the percentage decrease in the coefficient of friction of aged Cu-Zn-12Ni alloy was about 24.4%. Due to high microhardness values for aged alloys the ploughing is not as easy as in case of cast alloys. The aged alloys tend to impose large resistance to the ploughing action by the asperities of the counter disc. The formation of debris is greatly restricted due to which the surface of alloys remain relatively smooth leading to low coefficient of friction values for aged alloys. In addition to this the lubricating properties of Zn due to its hexagonal closed packed structure also contributes in the reduction of coefficient of friction.

3.4 Wear Rate

The wear rate of cast Cu-Zn-xNi alloys was studied for varying load (25 N to 100 N) and sliding velocity (0.314 m/s to 1.256 m/s) conditions. In addition to this the effect of heat treatment was also studied and compared with the values of cast alloys wear rate.

3.4.1 Effect of Load

The effect of Ni content on wear rate of cast Cu-Zn-xNi alloys plotted as a function of varying load is presented in the Figure 6. The wear rate values for Cu-Zn-4Ni alloy will be studied first followed by other two alloys obtained for varying loads from 25 N to 100 N. The Cu-Zn-4Ni alloy showed increase in the wear rate with increasing load and as seen from the figure for 25 N load, the wear rate was 55×10^{-3} mm^3/m. When the load was increased from 25 N to 50 N, the wear rate value increased to 57×10^{-3} mm^3/m. The percentage increment in the wear rate when load was increased was about 3.6%. Similarly when the load was increased to 75 N and 100 N, the wear rate increased to 61×10^{-3} mm^3/m and 63.5×10^{-3} mm^3/m respectively. Compared to 25 N, the increment in the wear rate was about 10.9% and 15.5% for 75 N and 100 N respectively. Overall for Cu-Zn-4Ni alloy higher wear rates was observed for higher load of 100 N and lower wear rate at lower load of 25 N. For the case of Cu-Zn-8Ni alloy wear rate was found to be increasing with increasing load from 25 N to 100 N. At 25 N load, the wear rate was 48×10^{-3} mm^3/m and when the load was increased from 25 N to 50 N, the wear rate show an sharp increase and the value obtained was 55×10^{-3} mm^3/m. The percentage increment in the wear rate when load was increased was about 14.5%. Similarly when the load was increased to 75 N and 100 N, the wear rate obtained were 60×10^{-3} mm^3/m and 62.5×10^{-3} mm^3/m respectively. Compared to 25 N, the increment in the wear rate was about 25% and 30.2% for 75 N and 100 N respectively. Overall, higher wear rate was observed at higher load of 100 N and lower value was obtained at lower load of 25 N. Finally in case of Cu-Zn-12Ni alloy case the wear rate was found to be increasing with increasing load. At 25 N and 50 N loads, the wear rate values were 40.5×10^{-3} mm^3/m and 42.5×10^{-3} mm^3/m respectively. The percentage increment in the wear rate when load was increased was about 4.9%. Similarly when the load was increased to 75 N and 100 N, the wear rate values obtained were 46.5×10^{-3} mm^3/m and 55×10^{-3} mm^3/m respectively. Compared to 25 N, the increment in the wear rate was about 14.8% and 35.8% for 75 N and 100 N respectively.

Overall higher wear rate value was observed at higher load of 100 N and low value was obtained at lower load of 25 N. The presence of Ni particles in the alloy tends to increase in microhardness for all alloys and as the Ni content increase from 4% to 12%, the microhardness also

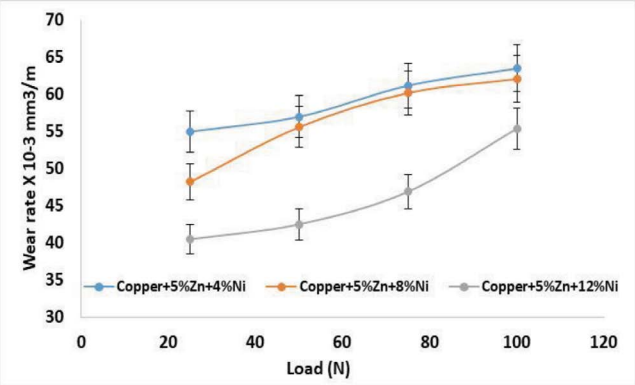

Figure 6. Effect of load on wear rate.

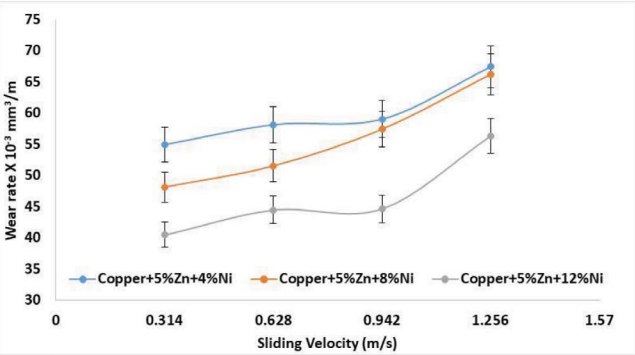

Figure 7. Effect of sliding velocity on wear rate.

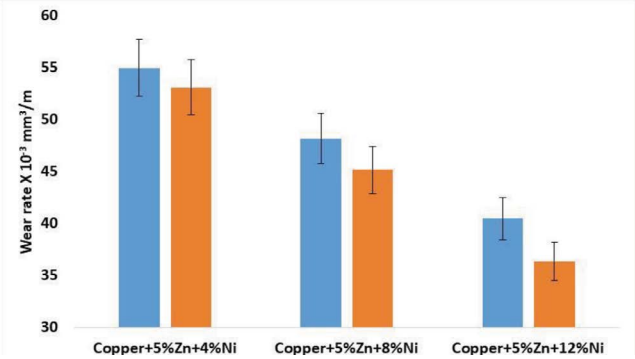

Figure 8. Effect of heat treatment on wear rate.

showed increasing in trend.In addition to this formation of fine dendrite grains and decreasing the secondary dendrite arm spacing also contributed to enhancement in the hardness. All these factors ensured that the Cu-Zn-12Ni alloy surface showed maximum resistance to the indentation being imposed by the asperities of the counter disc. The increase in wear resistance of Cu-Zn-12Ni alloy due to increase in microhardness is exact trend as described the Archard's equation (Toulfatzis *et al.*, 2016).

3.4.2 Effect of Sliding Velocity

The influence of Ni content on the wear rate of cast Cu-Zn-xNi alloys is depicted in Figure 7 as a function of sliding velocity. The wear rates of the Cu-Zn-4Ni alloy will be investigated first, followed by the wear rates of the other two alloys obtained at sliding speeds ranging from 0.314 m/s to 1.256 m/s. The wear rate of the Cu-Zn-4Ni alloy increased with increasing sliding velocity, and as seen in the figure with a 25 N load, the wear rate was 5510-3 mm3/m. The wear rate value increased to 57 x10^{-3} mm^3/m when the sliding velocity was raised from 0.314 to 0.628 m/s. When sliding velocity was increased, the wear rate increased by approximately 3.6 percent. Similarly, increasing the sliding velocity to 0.942 m/s or 1.256 m/s raised the wear rate to 59.5x10^{-3} mm^3/m and 68 x10^{-3} mm^3/m, respectively. In comparison to 0.314 m/s, the wear rate increased by approximately 8.2 percent and 23.6 percent at 0.942 m/s and 1.256 m/s, respectively. Overall, the Cu-Zn-4Ni alloy had a low wear rate at a sliding velocity of 0.314 m/s and a high wear rate at a sliding velocity of 1.256 m/s. The Cu-Zn-8Ni alloy exhibited an increase in wear rate with increasing sliding velocity, and as shown in the figure, the wear rate was 48 x10^{-3} mm^3/m at 0.314 m/s sliding velocity. The wear rate was increased to 51 x10^{-3} mm^3/m when the sliding velocity was raised from 0.314 to 0.628 m/s. When sliding velocity was increased, the wear rate increased by approximately 6.3 percent. Similarly, increasing the sliding velocity to 0.942 m/s or 1.256 m/s increased the wear rate to 57 x10^{-3} mm^3/m and 66 x10^{-3} mm^3/m, respectively. In comparison to 0.314 m/s, the wear rate increased by approximately 18.7% and 37.5 percent at 0.942 m/s and 1.256 m/s, respectively. Overall, the Cu-Zn-8Ni alloy had a low wear rate at a sliding velocity of 0.314 m/s and a high wear rate at a sliding velocity of 1.256 m/s. Finally, for the Cu-Zn-12Ni alloy, the wear rate rose with increasing sliding velocity, reaching 40.5 x10^{-3} mm^3/m at 0.314 m/s. The wear rate value increased to 44.5 x10^{-3} mm^3/m when the sliding velocity was raised from 0.314 to 0.628 m/s. When sliding velocity was increased, the wear rate increased by approximately 9.8 percent. Similarly, increasing the sliding velocity to 0.942 m/s or 1.256 m/s increased the wear rate to 45 x10^{-3} mm^3/m and 56 x10^{-3} mm^3/m, respectively. In comparison to 0.314 m/s, the wear rate increased by approximately 11.1 percent and 38.2 percent at 0.942 and 1.256 m/s, respectively. Overall, the Cu-Zn-12Ni alloy had a low wear rate at a sliding velocity of 0.314

m/s and a high wear rate at a sliding velocity of 1.256 m/s. Due to the increase in hardness caused by the increase in Ni content from 4% to 12%, the wear resistance increased as well, as well specified by Archard's equation (Kim *et al.*, 2012).

3.4.3 Effect of Heat Treatment

The effect of ageing on wear rate of cast Cu-Zn-xNi alloys was studied and obtained value as function of Ni content is presented in the Figure 8. The cast Cu-Zn-4Ni alloy showed wear rate value of 55×10^{-3} mm^3/m and after ageing process the value was decreased to 53×10^{-3} mm^3/m. When compared with the wear rate of cast alloy, the aged alloy showed 3.6% decrement in the value. On the other hand, the wear rate of cast and aged Cu-Zn-8Ni alloy were found to be 48×10^{-3} mm^3/m and 45×10^{-3} mm^3/m respectively. Compared with cast alloy the percentage decrease in the wear rate of aged Cu-Zn-8Ni alloy was about 6.25%. Finally in case of cast and aged Cu-Zn-12Ni alloy, the wear rate values were 40.5×10^{-3} mm^3/m and 36×10^{-3} mm^3/m respectively. Compared with cast alloy the percentage decrease in the coefficient of friction of aged Cu-Zn-12Ni alloy was about 11.1%. Along with decrease is secondary dendrite arm spacing and presence of Cu_2NiZn precipitates the microhardness of aged alloys was considerably higher than cast alloys due to which they exhibited higher resistance to wear.

3.5 Worn Surface Analysis

The worn surface analysis of alloys at lower load of 25 N and higher load of 100 N were carried out using SEM and are presented in the Figure 9 (a) – (f). At lower load of 25 N, all the alloys as presented in the Figure 9 (a), (b) and (c) showed parallel grooves running along sliding direction. However, with the increasing Ni content the number of parallel grooves decreased. The dominant mechanism for lower load was abrasion with some contribution by adhesion. At higher loads the number of parallel grooves increased in number and their depth was also higher than that observed for lower loads.

This observation is well in line with higher wear rates observed for higher loads for all alloys. However the Cu-Zn-12Ni alloy worn surface as shown in Figure 9 (c) and (f) showed less number of abrasive grooves and their depth was also less. This is due to the high microhardness possessed by the alloy and higher resistance imposed to indentation of asperities of the counter disc. The dominant mechanism for higher loads was abrasion with some contribution by adhesion which is similar observations made in case of lower loads.

The worn surface analysis of alloys at lower sliding velocity of 0.314 m/s and higher sliding velocity of 1.256 m/s are presented in the Figure10 (a) – (f). At lower sliding velocity of 0.314 m/s, all the alloys except Cu-Zn-12Ni alloy as presented in the Figure 10 (a) and (b) showed parallel grooves running along sliding direction. The Cu-Zn-12Ni alloy showed removal of material in the form of flakes as seen in the Figure 10 (c). The dominant mechanism for lower sliding velocity of 0.314 m/s was abrasion for Cu-Zn-4Ni and Cu-Zn-8Ni alloy while for Cu-Zn-12Ni alloy it was delamination. At higher sliding velocity of 1.256 m/s the number of parallel grooves increased in number and their depth except for Cu-Zn-12Ni alloy. This observation is well in line with higher wear rates observed for higher sliding velocity of 1.256 m/s for all alloys. However, the Cu-Zn-12Ni alloy worn surface as presented in the Figure 10 (f) showed removal of material in the form of flakes and their depth was considerably higher when compared to what observed for lower sliding velocity of 0.314 m/s (Figure 10 (c)). The dominant mechanism observed at higher sliding velocity of 1.256 m/s for Cu-Zn-4Ni and Cu-Zn-8Ni alloys was abrasion while delamination wear mechanism was observed for Cu-Zn-12Ni alloy.

4. Conclusions

The conclusions drawn from the current work as provided below:

- The microstructure analysis of cast and aged samples revealed α-phase (copper) and solid zinc solutions, but Cu_2NiZn precipitates were observed in aged samples.
- For both cast and aged conditions, the microhardness of Cu-Zn-xNi alloy increased with increasing Ni content. The main reason for the increase in microhardness was a significant decrease in secondary dendrite arm spacing with increasing Ni content.
- The coefficient of friction yielded mixed results, as increasing the load resulted in a decrease in the coefficient of friction for all alloys, whereas increasing the sliding velocities resulted in an increase in the friction coefficient.
- The wear rate was found to be increasing for both increasing load and sliding velocity conditions.

25N **100N**

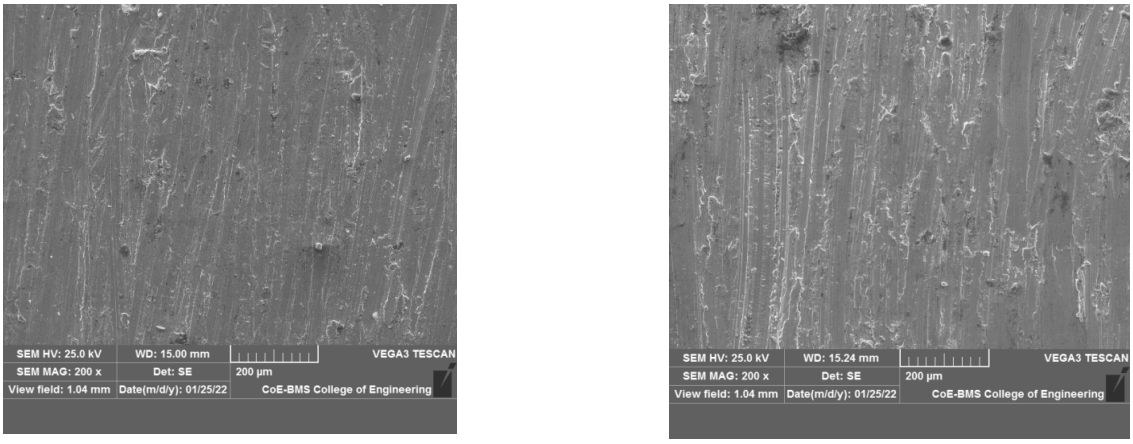

(a) **(b)**

Copper+5%Zn+4%Ni

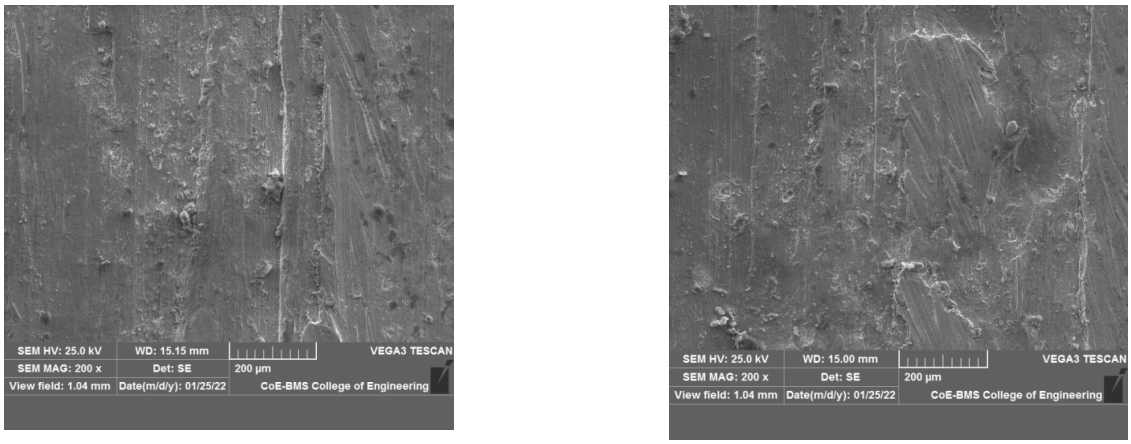

(c) **(d)**

Copper+5%Zn+8%Ni

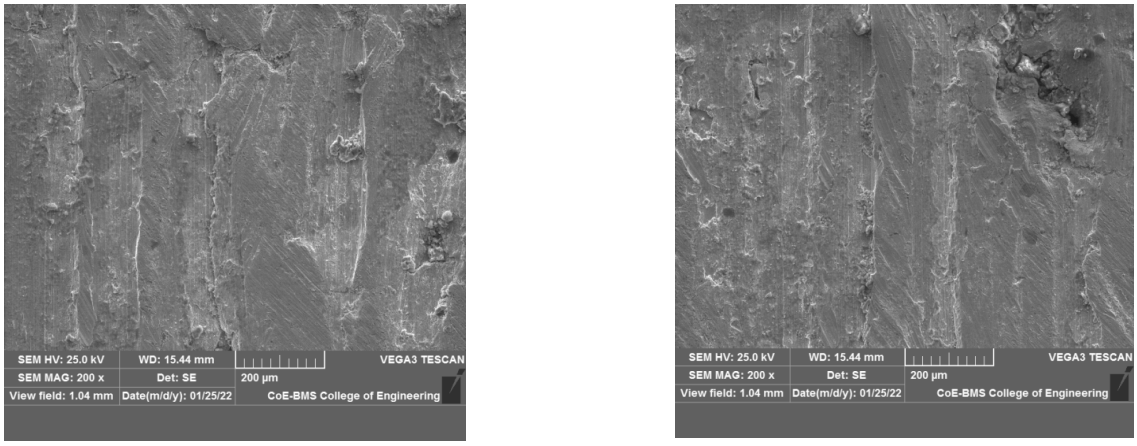

(e) **(f)**

Copper+5%Zn+12%Ni

Figure 9. (a-f) SEM of worn-out surfaces at different loads.

0.314m/s

1.256m/s

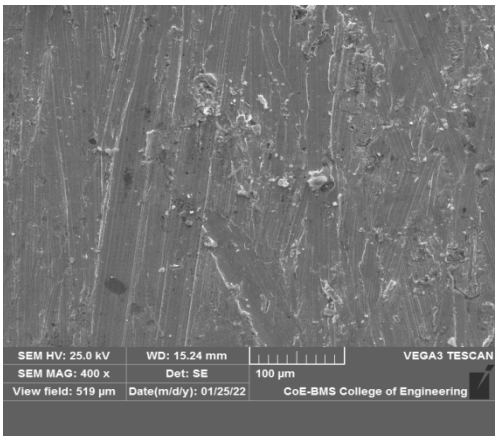

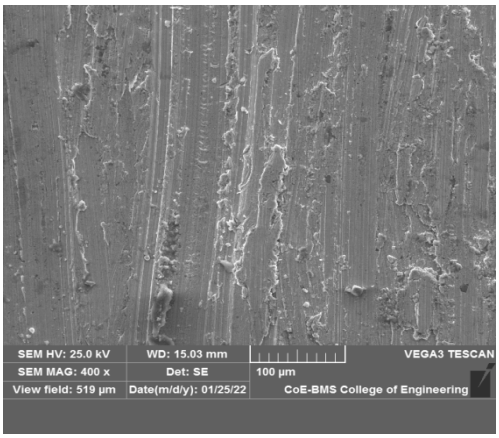

(a) **(b)**

Copper+5%Zn+4%Ni

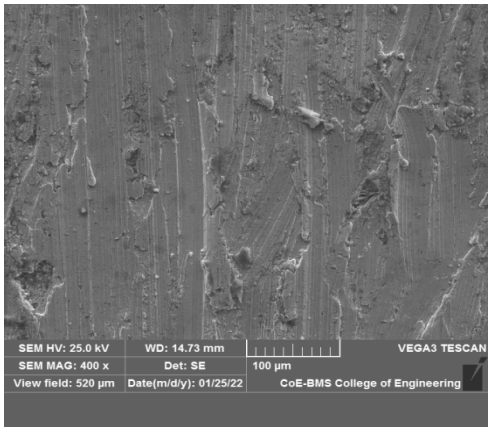

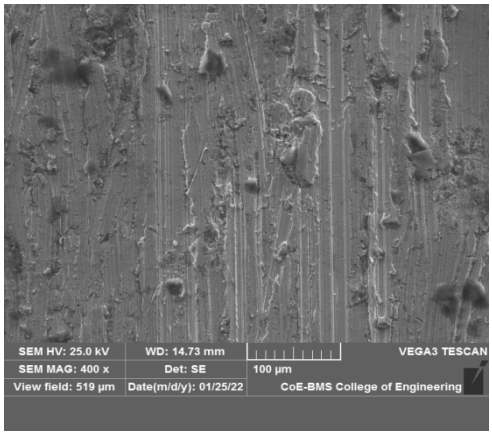

(c) **(d)**

Copper+5%Zn+8%Ni

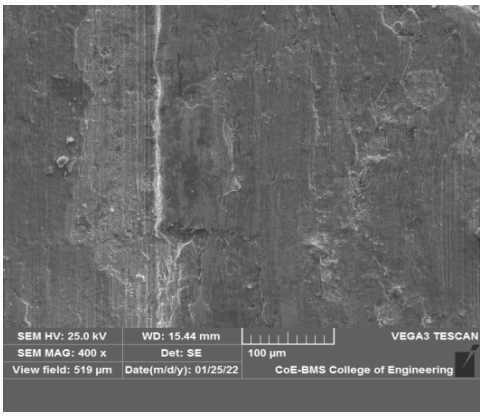

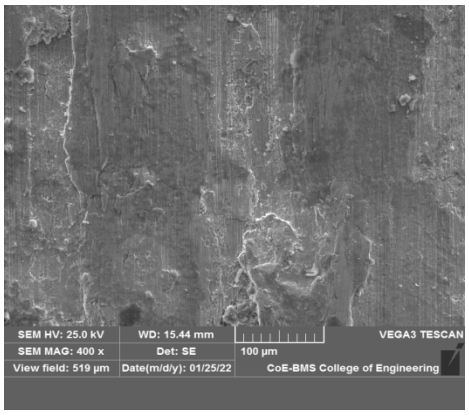

(e) **(f)**

Copper+5%Zn+12%Ni

Figure 10. **(a-f)** SEM of worn surfaces at different sliding velocities.

However, the Cu-Zn-12Ni alloy showed lower wear rate values in all cases.

- For lower and higher loads and sliding velocities, the worn surface analysis revealed that abrasion was the dominant mechanism.

5. References

1. Freudenberger J., & Warlimont H. (2018). Copper and copper alloys. In: W. Martienssen, H. Warlimont (Eds.), Springer Handbook of Materials Data, Springer Nature Switzerland AG, 293-301. https://doi.org/10.1007/978-3-319-69743-7_12
2. Davis J. R. (2001). Copper and Copper Alloys, ASM Specialty Handbook, ASM International, Materials Park, OH.
3. Stewart M. (2021). Materials of construction, In: Surface Production Operations, Volume 5: Pressure Vessels, Heat Exchangers, and Aboveground Storage Tanks: Design, Construction, Inspection, and Testing, Elsevier Inc., 61–92. https://doi.org/10.1016/B978-0-12-803722-5.00003-3. PMCid:PMC8444439
4. Prasad B. K. (1997). Dry sliding wear response of some bearing alloys as influenced by the nature of microconstituents and sliding conditions. *Metallurgical and Materials Transactions A, 28*, 809–815. https://doi.org/10.1007/s11661-997-0067-9
5. Davim J. P. (2000). An experimental study of the tribological behaviour of the brass/steel pair. *Journal of Materials Processing Technology*, *100*, 273–277. https://doi.org/10.1016/S0924-0136(99)00491-4
6. Sadykov F. A., Barykin N. P., & Aslanyan I. R. (1999). Wear of copper and its alloys with submicrocrystalline structure. *Wear,* 225–229, 649–655. https://doi.org/10.1016/S0043-1648(98)00374-3
7. Davim J. P. (2000). An experimental study of the tribological behaviour of the brass/steel pair. *Journal of Materials Processing Technology, 100*, 273–277. https://doi.org/10.1016/S0924-0136(99)00491-4
8. Unlu B. S. (2009). Investigation of tribological and mechanical properties of metal bearings. *Bulletin of Materials Science, 32*, 451–457. https://doi.org/10.1007/s12034-009-0066-0
9. Kucukomeroglu T, & Kara L. (2014). The friction and wear properties of CuZn39Pb3 alloys under atmospheric and vacuum conditions, *Wear*, *309*, 21–28. https://doi.org/10.1016/j.wear.2013.10.003
10. Moshkovich A., Perfilyev V., Lapsker I., & Rapoport L. (2014) Friction, wear and plastic deformation of Cu and α/β brass under lubrication conditions, *Wear, 320*, 34–40. https://doi.org/10.1016/j.wear.2014.08.016
11. Chen W., Jia Y., Yi J., Wang M., Derby B., & Lei Q. (2017). Effect of addition of Ni and Si on the microstructure and mechanical properties of Cu-Zn alloys. *Journal of Materials Research*, *32*, 3137–3145. https://doi.org/10.1557/jmr.2017.145
12. Wang P., Jie J., Tong L., Li T. (2019). Study of the mechanical, structural, and electrical properties and annealing effect of a Cu-30Zn-1Ni-0.2Si alloy fabricated using cryogenic rolling. *Materials Research Express, 6*(11). https://doi.org/10.1088/2053-1591/ab49cd
13. Joszt K., Stobrawa J., & Zaborowski G. (2013). Ordering process in Cu-18Ni-26Zn alloy. *Metals Technology*, *7*, 424–427. https://doi.org/10.1179/030716980803286775
14. Moussa M. E., & Ibrahim K. M. (2022). Effect of ultrasonic vibration treatment on microstructure, tensile properties, hardness and wear behaviour of brass alloy. *International Journal of Metalcasting.* https://doi.org/10.1007/s40962-021-00748-8
15. Knych T., Smyrak B., & Walkowicz M. Research on the influence of the casting speed on the structure and properties of oxygen-free copper wires, AGH University of Science and Technology, Poland; 2011.
16. Yan Z., Chen M., Yang J., Yang L., & Gao H. (2013). Grain refinement of CuNi10Fe1Mn alloy by SiC nanoparticles and electromagnetic stirring. Materials and Manufacturing Processes, *28*, 957–961. https://doi.org/10.1080/10426914.2013.763971
17. Bagherian E., Fan Y., Cooper M., Frame B., Abdolvand A. (2016). Effect of water flow rate, casting speed, alloying elements and pull distance on tensile strength, elongation percentage and microstructure of continuous cast copper alloys. *Metallurgical Research &Technology*, *113*, 308. https://doi.org/10.1051/metal/2016006
18. Reis B. P., Franca R. P., Spim J. A., Garcia A., da Costa E. M., & Santos C. A. (2013). The effects of dendritic arm spacing (as-cast) and aging time (solution heat-treated) of Al-Cu alloy on hardness. *Journal of Alloys and Compounds, 549*, 324–335. https://doi.org/10.1016/j.jallcom.2012.09.041
19. Jang H. W., & Hong J-W. (2020). Influence of zinc content on the mechanical behaviors of Cu-Zn alloys by molecular dynamics. *Materials (Basel), 13*(9), 2062. https://doi.org/10.3390/ma13092062. PMid:32365697. PMCid:PMC7254338
20. Igelegbai E. E., Alo O. A., Adeodu A. O., & Daniyan I. A. (2016). Evaluation of mechanical and microstructural properties of α-brass alloy produced from scrap copper and zinc metal through sand casting process. *Journal of*

Minerals and Materials Characterization and Engineering, *5*(1), 18–28. https://doi.org/10.4236/jmmce.2017.51002

21. Toulfatzis A. I., Pantazopoulos G. A., & Paipetis A. S. (2016). Microstructure and properties of lead-free brasses using post-processing heat treatment cycles. *Materials Science and Technology*, *32*, 1771–1781. https://doi.org/10.1080/02670836.2016.1221493
22. Purcek G., Savaskan T., Kucukomeroglu T., Murphy S. (2002). Dry sliding friction and wear properties of zinc-based alloys. *Wear*, *252*, 894–901. https://doi.org/10.1016/S0043-1648(02)00050-9
23. Kim H. S., Kim W. Y., & Song K. H. (2012). Effect of post-heat treatment in ECAP processed Cu-40%Zn brass. *Journal of Alloys and Compounds*, *536*, S200–S203. https://doi.org/10.1016/j.jallcom.2011.11.079